Available online at www.sciencedirect.com
ScienceDirect
Cement and Concrete Research 37 (2007) 242–250
Cement and Concrete Research

Study on the flexural fatigue performance and fractal mechanism of concrete with high proportions of ground granulated blast-furnace slag

Li-Ping Guo *, Wei Sun, Ke-Ren Zheng, Heng-Jian Chen, Bo Liu

College of Materials Science & Engineering, Southeast University, Nanjing 210096, China

Received 26 August 2005; accepted 2 November 2006

Abstract

The flexural fatigue performance of concretes with 50% and 80% proportions of ground granulated blast-furnace slag (ab. ggbs) by mass of total cementitious materials in concrete has been investigated. The effect of different proportions of ggbs on concrete fatigue performance was investigated by experiments and was estimated by the fractal theory from five aspects, i.e. the 1D fractal dimensions of critical surface cracks, the prediction area of fractured profiles, the ratios between the area of debonded coarse aggregates and the *Euclidean* area of fractured profile, fracture energy modified by fractal theory, and the brittleness index. In order to estimate these fractal parameters on-line, the grey model GM (1, 1) was employed. Those experimental and numerical results show that the brittleness of concrete is impaired by the incorporation of ggbs, which contribute to higher fracture energy and more complicated characteristics on fractured profiles of concrete. Therefore, potential hydration and pozzolanic effect of ggbs in matrix prolong the fatigue life of concrete comparing with those of concrete without them. The fractal theory and grey model are novel approaches to present quantitatively the flexural fatigue performance of concrete.
© 2006 Elsevier Ltd. All rights reserved.

Keywords: Ground granulated blast-furnace slag; High proportion; Concrete; Flexural fatigue; Fractal theory; Grey model; Surface macro-crack; Fractured profile; Brittleness; Fracture energy

1. Introduction

The mass fraction of ground granulated blast-furnace slag (ab. ggbs) in concrete engineering is less than 50% mass of total cementitious materials because the higher proportion of ggbs can impair the compressive strength of hardened concrete at the 28-day ages. However, it was found that incorporation of ggbs as cementitious materials in concrete can decrease the demand of Portland cement, dry and autogenous shrinkage in early ages, carbonation depth and effect of sulfate corrosion on concrete damage as well as improve the strength in early ages and workability of fresh concrete slurry. And the cost of concrete with ggbs is lower than normal concrete and the chemical composites of slag grain are stabler than fly ash. Recently, the concrete with high proportion of ggbs and superplasticizer at lower water-to-binder ratio can hold equal or higher strength than normal concrete. For some concrete engineering, e.g. highway slab and marine structures, etc., ggbs is one of popular raw materials as a part of cementitious materials in the concrete matrix. However, these projects are usually subjected to cyclic loading until failure. Therefore, the fatigue performance of concretes with high dosage of ggbs was investigated and estimated based on fractal theory.

Fractal geometry is particularly useful in characterizing the irregular objects which are not susceptible to regular *Euclidean* analysis. A *fractal* domain is a mathematical set with a non-integer dimension [1]. Fractal theory focuses on stochastic image existing universally in nature with self-similar characteristic, the fractal parameters can describe the inherent law of natural images and estimate the various effects on these ones [2]. Therefore, fractal theory was utilized to investigate the properties of concrete triumphantly, such as crack generation, size-effect of strength, grading of aggregates, etc. Since the fractured profile of concrete may be modeled through a fractal set, then the macro-performance and the mechanical properties of concrete can be connected closely with fractal dimensions. As the fractal dimension is larger, the appearances of crack path and fractured profile are more complicated [3].

* Corresponding author. Tel.: +86 25 8165 4819; fax: +86 25 5209 0667.
E-mail address: guoliping691@163.com (L.-P. Guo).

0008-8846/$ - see front matter © 2006 Elsevier Ltd. All rights reserved.
doi:10.1016/j.cemconres.2006.11.009

The experimental methods and preparation of specimen were described in Section 2. The experimental results were summed up in Section 3. Several fractal parameters established to indicate these performances of concrete with ggbs were introduced in details in Section 4. Furthermore, the grey model GM (1, 1) was employed to inspect and estimate the experimental results on-line. The experimental results show that the brittleness and fracture energy of concrete under same cyclic stress level are improved by incorporation with more than 50% proportion of ggbs by mass of total cementitious materials.

2. Experimental preparation

2.1. Raw materials

The Chinese standard P·II 42.5 Portland Cement (PC), a commercial naphthalene superplasticizer agent, and S95 grade of ggbs were incorporated into matrix as cementitious materials. The chemical and physical characteristics of cementitious materials were presented in Tables 1 and 2, respectively.

2.2. Mix proportion and specimens

The crushed basalt with a maximum diameter of 20 mm and the natural river sand with maximum diameter of 3.5 mm are mixed into specimens as coarse and fine aggregate, respectively. The fineness module of sand is 2.85. The mix proportions of three concrete series were shown in Table 3. Among that, the original designed concrete strength grade was C50, and the slump of fresh concrete was controlled between 80 mm and 120 mm by superplasticizer agent. The concrete was cast in metal mould and subjected to air curing at atmosphere pressure. The demoulded specimens were kept in curing room with 20± 2 °C and more than 90% relative humidity for 7 days. Then, they were removed outside and covered by wet straw mat for more than 90 days. The size of the prism is 100 mm × 100 mm × 400 mm and the effective span on load set-up is 300 mm. The fatigue experiments were carried out in lab with environment of 25 °C and 60% relative humidity. Three flexural specimens of each series were chosen for static flexure strength and others were for flexure fatigue tests under various stress levels.

2.3. Fatigue parameters

The static flexure strength and flexure fatigue test were carried out by PWS-100B flexure fatigue testing machine equipped for closed-loop system and the MTS fatigue controller. Its maximal dynamic load is ±100 kN. The prisms were subjected to unidirectional cyclic loading by means of a four-point bending test (Fig. 1). Each of them was loaded by applying two cyclic forces on the cross-sections at 1/3 and 2/3 of the span. The flexure fatigue tests were carried out by a hydraulic press with constant amplitude of sinusoidal load. The frequency of cyclic loading is 10 Hz. Six nominal stress levels, S, were chosen for each series, i.e. 0.90, 0.85, 0.80, 0.75, 0.70 and 0.65. A constant load ratio of 0.1 between minimum and maximum cyclic stresses was used in the present test program. All these data were input to the matched MTS controller before beginning of the flexural fatigue experiments.

Table 1
Chemical compositions of cementitious materials

Materials	SiO_2	MgO	Al_2O_3	Fe_2O_3	CaO	Na_2O	SO_3	K_2O
PC	21.68	0.81	5.64	4.22	64.89	0.20	1.00	0.76
ggbs	32.07	9.30	14.68	0.97	35.81	0.64	2.51	0.53

Table 2
Major physical properties of cementitious materials

Parameters		PC	ggbs
Density/kg m^{-3}		3115	2860
Specific surface area/m^2 kg^{-1}		309	372
Loss on ignition/%		1.04	0.58
Granularities (vol.%)	0.3–1 μm	5.22	6.02
	1–10 μm	23.88	28.84
	10–50 μm	59.43	54.57
	50–100 μm	10.85	9.94
	100–150 μm	0.62	0.63

3. Experimental results

Since three series of samples were cured more than 90 days, the ratio of static flexural strength and compressive strength was about 0.1. The static flexural strength and flexure fatigue life of three series were presented in Tables 4 and 5, respectively. It is clear that incorporation of ggbs in matrix impaired the static flexural strength of concrete with the same water-to-binder ratio.

Based on the results shown in the Table 5, the relevant experimental results are typically expressed in terms of S~lgN_f curves in Fig. 2. It is clear that the fatigue life of C50-ggbs50 is the longest in three series and those of C50-PC is the shortest as stress level is 0.80 or more. However, as stress level is lower than 0.80, the fatigue life of C50-ggbs80 is the longest among three mixes. As stress level is 0.65, C50-PC fractures at about 2×10^6 circles, whereas the fatigue life of concretes with ggbs is all extended 2×10^6 circles. The reason is that the bond strength of interface transition zone (ab. ITZ) between coarse aggregate and matrix is weakened by incorporation of ggbs with a specific surface area of 372 m^2/kg [4]. The potential reason is that the grain size of ggbs in this work is similar to those of Portland cement (shown in Table 2) and the elastic modulus of ggbs grain is lower than those of cement grain [5]. Moreover, the effect of ggbs on bond strength of ITZ in concrete is more negative as increasing the mass fraction of ggbs in matrix. As we know the flexural strength of concrete is more sensitive to the

Table 3
Mix proportions of concretes

Series	PC (kg/m^3)	ggbs (kg/m^3)	w/b	Aggregate/ binder	S and ratio	Superplasticizer (kg/m^3)
C50-PC	460	0	0.35	2.4	0.38	2.3
C50-ggbs50	230	230	0.35	2.4	0.38	2.3
C50-ggbs80	98	362	0.35	2.4	0.38	2.3

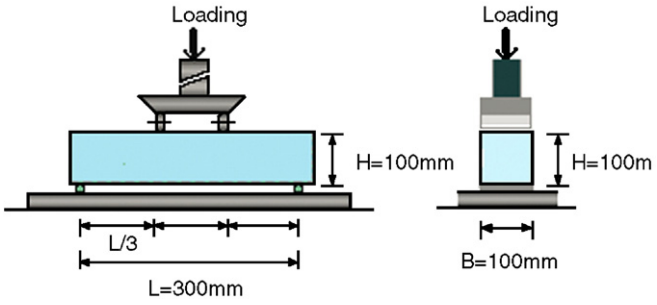

Fig. 1. The loading configuration and dimensions of specimen.

performance of this ITZ than compressive strength [5], then the effect of ggbs on flexural fatigue life of concrete is more obvious. However, since the bond strength of this macro-ITZ is weakened, the micro- and macro-cracks would generate and propagate mostly in this zone. That means the crack path would be more zigzag before concrete failure. Therefore, the fatigue life of concrete with ggbs is longer than those of concrete without them.

4. Fractal mechanism and grey model prediction

Two methods were presented to investigate the fatigue mechanisms of concrete. The grey model GM (1, 1) was employed to predict fatigue performance of specimens at different stress levels and estimate the experimental results. The fractal theory is cited to present the fatigue performance of concrete after failure. The fractal theory is an efficient bridge tool to connect the mechanical performance and microstructure of concrete, which are influenced by curing ages and mass fraction of ggbs in matrix. The fractal dimensions of surface cracks and crack profiles of fractured concretes will vary with different stress levels and different proportions of ggbs in matrix. Their definitions and deducing processes were described as follows.

4.1. Introduction of GM (1, 1)

The grey model theory was originally presented by Deng in 1989 [6–8]. It mainly analyzes the uncertain and insufficient information in a system to estimate its condition, to forecast and to make decision. The grey system puts each stochastic variable as a grey quantity that changes within a given range; however, it relies on a series of novel method to deal with those grey quantities [9]. The critical different between grey model with statistics is that the former unearths directly the intrinsic law in original faulty data rather than processed ones and the prediction work can be done accurately based on only four data rather than tens of them. It uses a first-order differential equation to deduce the model and the calculating results can be easily computed by MATLAB program. The model process is present as follow [9]:

For an initial time sequence

$$X^{(0)}(i) = \left\{x^{(0)}(i), i = 1,2,\ldots,n\right\} \tag{1}$$

Where $x^{(0)}(i)$ is the time series data at time i, n must be equal to or more than 4.

By accumulating each two data in sequence $X^{(0)}$, a new sequence $X^{(1)}$ is set up. It is useful to provide the middle message that is helpful in modeling and to weaken the variation tendency, i.e.

$$X^{(1)}(k) = \left\{x^{(1)}(k), k = 1,2,\ldots,n\right\} \tag{2}$$

where, $x^{(1)}(k) = \sum_{i=1}^{k} x^{(0)}(i), k = 1,2,\ldots,n$

Ordering $x^{(0)}(1)=x^{(1)}(1)$, the first-order differential equation of $X^{(1)}$ is the following

$$\frac{dX^{(1)}}{dt} + aX^{(1)} = u \tag{3}$$

where, $\hat{a}=\{a,u\}^T$. Then the $\frac{dX^{(1)}}{dt}$ is substituted by $X^{(0)}$ and the above equation is

$$X^{(0)}(k) + aZ^{(1)}(k) = u \qquad k = 2,3,\ldots,n \tag{4}$$

and

$$Z^{(1)}(k) = \frac{1}{2}\left(x^{(1)}(k) + x^{(1)}(k+1)\right) \qquad k = 1,2,\ldots,(n-1) \tag{5}$$

which can be defined as

$$Y_n = B\hat{a} \tag{6}$$

wherein,

$$\boldsymbol{Y}_n = \left\{x^0(2), x^{(0)}(3), \ldots, x^{(0)}(n)\right\}^T \tag{7}$$

$$\mathbf{B}^T = \begin{bmatrix} -Z^{(1)}(2) & -Z^{(1)}(3) & \ldots & -Z^{(1)}(n) \\ 1 & 1 & \ldots & 1 \end{bmatrix} \tag{8}$$

$$\hat{a} = \{a,u\}^T = (\mathbf{B}^T\mathbf{B})^{-1}\mathbf{B}^T\boldsymbol{Y}_n \tag{9}$$

Table 4
Average values of static flexural strength

Specimens	C50-PC	C50-ggbs50	C50-ggbs80
Mean values (MPa)	7.65	7.14	5.87

Table 5
Average cycles of flexural fatigue life (N_f)

Stress levels	C50-PC	C50-ggbs50	C50-ggbs80
0.90	68	114	78
0.85	1015	1355	620
0.80	4212	9506	5904
0.75	50,433	43,679	59,971
0.70	413,988	469,963	565,779
0.65	2,000,801	$>2\times10^6$	$>2\times10^6$

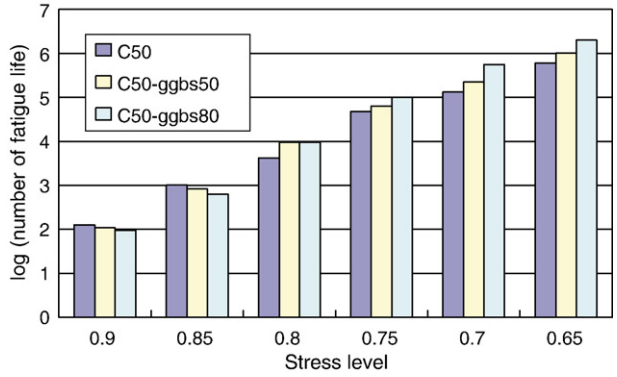

Fig. 2. S~lgN_f histograms of three series.

In Eq. (6) $\hat{a}$ is the unknown coefficient, $\boldsymbol{Y}_n$ and $\mathbf{B}$ are the constant vector and the accumulated matrix respectively.

Finally, substituting parameters in Eq. (6) with Eqs. (5)–(9), the forecasting equation of GM (1, 1) is available given

$$\hat{x}^{(1)}(k+1) = \left(x^{(0)}(1) - \frac{u}{a}\right)e^{-ak} + \frac{u}{a} \tag{10}$$

Where $\hat{x}^{(1)}(k+1)$ is the accumulated predicted value of $x^{(1)}(k+1)$ at time $(k+1)$. Therefore, the real predicted value of $x^{(0)}(k+1)$ at time $(k+1)$ is

$$\hat{x}^{(0)}(k+1) = \hat{x}^{(1)}(k+1) - \hat{x}^{(1)}(k)\ , \quad k = 0,1,2,... \tag{11}$$

Based on former only four initial experimental data, the following ones would be predicted by GM(1, 1).

4.2. Fractal dimensions of surface macro-cracks

The zigzag content of surface macro-crack may reflect the essential that the influence of different percentages of ggbs and different stress levels on the fatigue properties of concrete. It is helpful to estimate these effects by fractal dimension of surface macro-crack. Because the fractal theory focuses on stochastic image existing universally in nature with self-similar characteristic, the fractal parameters can describe the inherent law of natural images and estimate the various effects on these ones. In this paper, the box-counting method is utilized to calculate the fractal dimension of critical surface crack. Firstly, the crack is covered with a rectangular mesh with different grid sizes, δ [2].

$$N = \frac{V^*}{\delta^{D_{1-d}}} \tag{12}$$

Where V^* is the hyper-volume of the fractal object. All of the samples were analyzed by mesh with 100×100 grids in the whole trace. The largest grid size is equal to the length of the whole trace and the smallest one was 1/100th of the whole trace. If a grid size smaller than 1/100th was used, each grid that makes up the trace would be detected, resulting in a fractal dimension estimate of zero [2]. By varying δ and counting the number of grids covered by traces, a logarithmic plot of $\log(N)$ versus $\log(1/\delta)$ can be drawn. Then the slope of their fitting line is the fractal dimension D_{1-d}. The experimental and GM (1, 1) prediction results were presented in Fig. 3.

The D_{1-d} results shown in Fig. 3 are consistent with [2]. It can be concluded that the fractal dimensions of C50-PC are the lowest among three mix concretes. With incorporation of ggbs in concrete, the surface macro-cracks become more complicated and their fractal dimensions are higher than those of concrete without ggbs.

4.3. Simplified fractal method for fractured profile area

The crack profiles of fractured concretes are coarse and anomalistic, but which have the statistical self-similar characteristics. The fractal dimensions that represent the coarseness content of crack profiles lie on the macro- and microscopic structures [10]. This parameter is important for fracture analysis of concrete engineering [10], and is a valid approach to estimate the fatigue mechanisms of concrete with ggbs.

4.3.1. Simplified method to calculate A_s

In [10,11], five methods to calculate the fractal dimension were concluded. However, the same disadvantage of these methods is

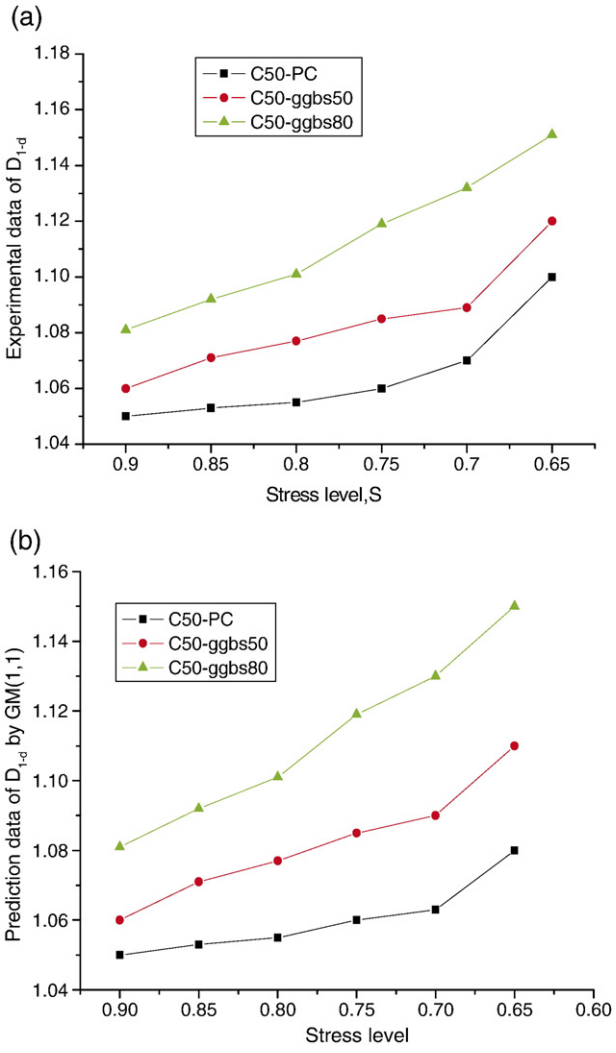

Fig. 3. D_{1-d} and stress level relations of three concrete series. (a) Experimental results; (b) GM (1, 1) prediction results.

the complex and nonstandard equipment used to measure fractal dimension. The experimental results in different literatures are different between each other. In order to overcome this defect, one simplified method was advanced in this paper.

The figure of surface crack is the outer token of internal structure of concrete. If using D_{1-d}, that is the mean value of fractal dimensions of four surface cracks on fractured specimen, to estimate real area A_s of crack profiles, it may be more convenient for the technicians in practice to compare the properties of concrete with different compositions. And may reduce the bothers brought out by different fractal approaches. Therefore, the simplified method to calculate the fractal dimension of surface crack on fractured sample is presented as follows.

The real length of a fractal curve is

$$L_S = L_0\left(\frac{\delta}{L_0}\right)^{1-D} \tag{13}$$

Wherein, L_0 is the *Euclidean* length, δ is the scale of the fractal set, D is the fractal dimension of this curve. H and B represent the *Euclidean* high and Euclidean breadth of specimen, respectively.

Similar to the Eq. (13), the real lengths of high and breadth of specimen can be rewritten as Eqs. (14) and (15). Where, D_H is the mean fractal dimension of surface crack path which is perpendicular to the principle stress vector, and D_B is the mean fractal dimension of surface crack path paralleling to the principle stress vector.

$$H_S = H\left(\frac{\delta}{H}\right)^{1-D_H} \tag{14}$$

$$B_S = B\left(\frac{\delta}{B}\right)^{1-D_H} \tag{15}$$

Similarly, the real area of fractured profile is defined based on fractal theory as

$$A_s = A\cdot\left(\frac{\delta}{A}\right)^{2-D_{2-d}} = HB\cdot\left(\frac{\delta}{HB}\right)^{2-D_{2-d}} \tag{16}$$

However, the accurate A_s is difficult to be calculated by normal methods. In order to simplify the calculation of A_s at fractured profile, A'_s is established as follow:

$$A'_s = H_S\cdot B_S = H\left(\frac{\delta}{H}\right)^{1-D_H}\cdot B\left(\frac{\delta}{B}\right)^{1-D_B} \tag{17}$$

If H is equal to B, the above equation can be rewritten to

$$\begin{aligned} A'_s &= H_S\cdot B_S \\ &= HB\left(\frac{\delta}{B}\right)^{2-(D_H+D_B)} \\ &= HB\left(\frac{\delta^2}{HB}\right)^{2-(D_H+D_B)}\cdot\delta^{(D_H+D_B)-2}\cdot H^{2-(D_H+D_B)} \\ &= A\left(\frac{\delta^2}{A}\right)^{2-(D_H+D_B)}\cdot\delta^{(D_H+D_B)-2}\cdot H^{2-(D_H+D_B)} \\ &= A_s\cdot\left(\frac{\delta}{H}\right)^{(D_H+D_B)-2} \end{aligned} \tag{18}$$

Then, the real area at fractured profile can be deduced to

$$A_s = A'_s\cdot\left(\frac{\delta}{H}\right)^{2-(D_H+D_B)} \tag{19}$$

4.3.2. Prediction results of A_s

After specimen fractures, the surface macro-crack paths were captured by digital camera and then calculate D_H and D_B by box-counting method. The value of δ selected in following equations is 5 mm, which is the same as the maximum diameter of sand in concrete. The value of H and B is 100 mm, respectively. Based on the Eq. (19), the prediction results of A_s were presented in Fig. 4.

The magnitude of A_s data in Fig. 4 was the same as the experimental results listed in [12].

The data of A_s vary with the stress level and proportions of ggbs in concrete. It is clearly that the fractal dimensions of C50-PC are the lowest among three concrete series. And A_s will become higher when playing down the stress levels. The growth rate of internal micro-cracks is slowed down by the incorporation of ggbs in the matrix.

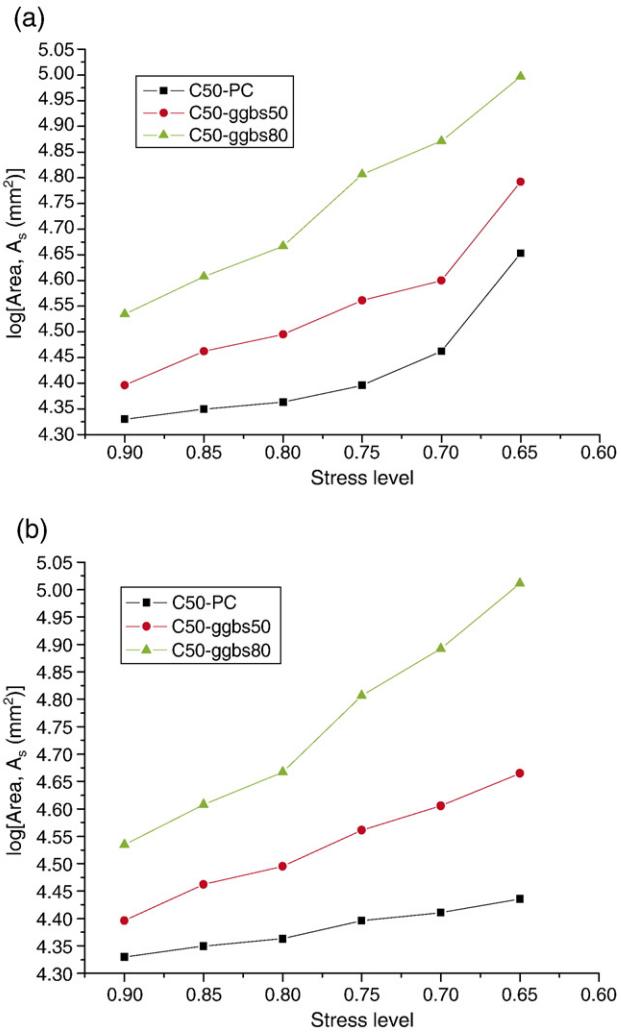

Fig. 4. log A_s and stress level relations of three concrete series. (a) Experimental results; (b) GM (1, 1) prediction results.

4.4. Definition of brittleness parameter

In order to present the brittleness of concrete, the above defined parameters A and A_s were cited to define this parameter, [13].

$$R_B = \frac{A}{A_s},\ R_B \in (0,1) \tag{20}$$

Substituting Eq. (20) with Eqs. (18) and (19) is

$$R_B = \frac{HB}{HB\left(\frac{\delta^2}{HB}\right)^{2-(D_H+D_B)}} = \left(\frac{\delta^2}{HB}\right)^{(D_H+D_B)-2},\ R_B \in (0,1) \tag{21}$$

where the value of δ is 5 mm corresponding to the maximum diameter of sand in concrete. The value of H and B is 100 mm, respectively.

The relationship of brittleness versus coarse content of fractured profile is inversely. While the concrete has higher brittleness, the coarse content of fractured profiles is higher and the fatigue life of concrete under flexural cyclic stress is longer. Contrarily, the shorter fatigue life is as a result of higher brittleness of specimen. By the experimental results of D_{1-d}, the brittleness data of three series of specimens were drawn in Fig. 5.

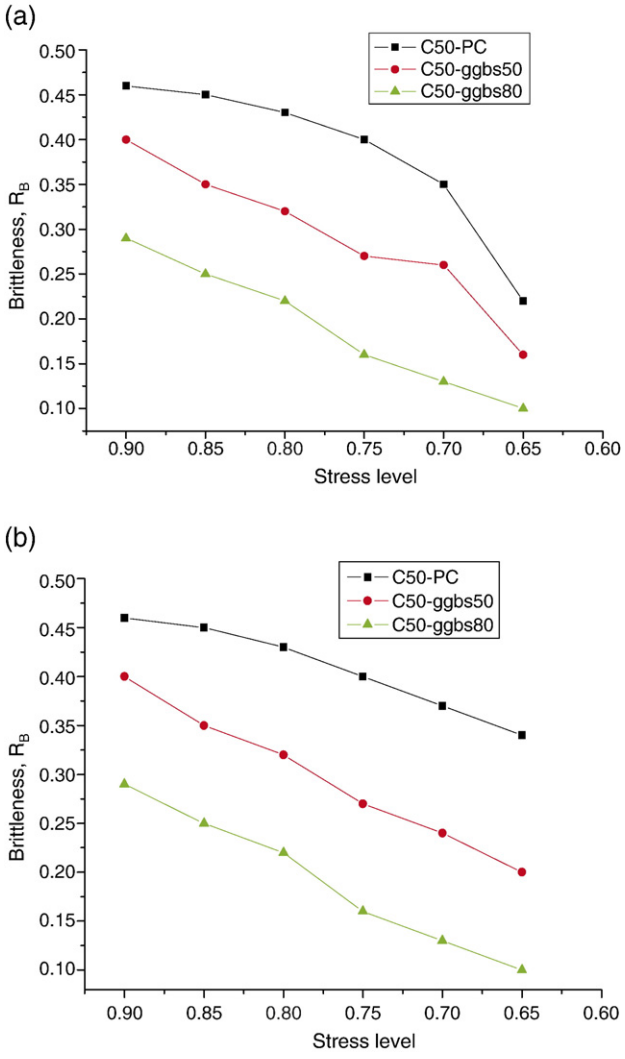

Fig. 5. Brittleness and stress level relations of three concrete series. (a) Experimental results; (b) GM (1, 1) prediction results.

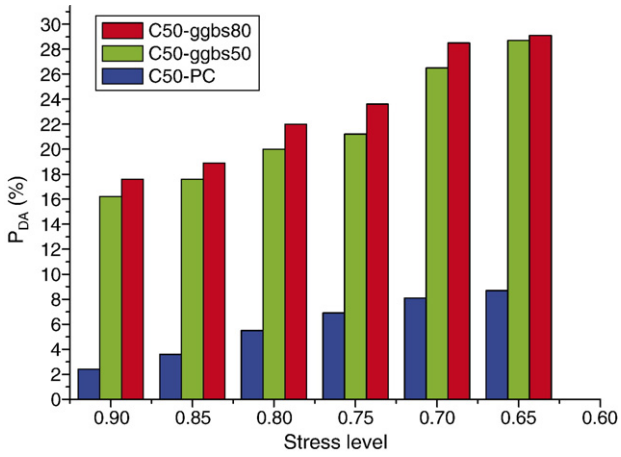

Fig. 6. P_{DA} and stress level relations of three concrete series.

It is indicated that the brittleness of samples under flexural fatigue stress is decreased when playing down the stress levels. At the same stress level, the brittleness of C50-ggbs50 and C50-ggbs80 is lower than C50-PC. Lower the stress level and lower the brittleness they have.

4.5. Projective area of coarse aggregates on fractured profile

It is well-known that coarse aggregate is the main composition in concrete. Its texture and strength will decide greatly the compressive strength and the failure mode of concrete. In this section, two fracture modes were appeared: one is the cracks along with the interface zone between the matrix and coarse aggregate, and the other is the cracks tips penetrate through the coarse aggregate to above matrix. If the concrete fractures in the first form, the coarse content of fractured profile will be decreased. Contrarily, the fractured profile will be rougher and its A_s will be larger. After checking the fractured profiles, the former fracture mode usually happens in C50-PC, and the latter mode is popular in C50-ggbs50 and C50-ggbs80.

Therefore, two parameters were established to present the performance of ITZ between coarse aggregate and matrix, i.e. P_A and P_{DA}. P_A is the ratio of projective area of total coarse aggregates on the fractured profiles to the projective *Euclidean* area of concrete cross-section. Similarly, P_{DA} is the ratio of projective area of debounded coarse aggregates on the fractured profiles to the projective *Euclidean* area of concrete cross-section.

The P_{DA} is a function of performance of ITZ between coarse aggregate and matrix. It can be used to present qualitatively the defect of microstructure around broken coarse aggregates. P_{DA} is controlled by the difference between bond strength of ITZ and tensile strength of matrix. In the [14], if the tensile strength of

matrix is lower than bond strength of ITZ between coarse aggregate and matrix, the micro-cracks propagate mainly along this zone. Whereas, the fracture mode is that the crack tips traverse the coarse aggregates and spread into matrix. The experimental result of P_A was 33% in three series of concrete. The experimental results of P_{DA} in three series of concretes were different with matrix and stress levels (illustrated in Fig. 6). The P_{DA} data of C50-PC are the lowest than others and less than 10%. However, those of C50-ggbs80 are higher than C50-ggbs50.

The experimental results in Fig. 6 show that the incorporation of ggbs with specific surface area of 372 m^2/kg weakened the bond strength of ITZ between coarse aggregate and matrix because more coarse aggregates on fractured profiles of concrete with ggbs were debonded during the cyclic loading. These results of P_{DA} are consistent with those of A_s and brittleness. The potential reason is that the grain size of ggbs in this work is similar to those of Portland cement (Shown in Table 2) and the elastic modulus of ggbs grain is lower than those of cement grain [5]. Therefore, the compacting and crack-resisting actions of ggbs with specific surface area of 372 m^2/kg in ITZ between coarse aggregate and matrix are not excellent.

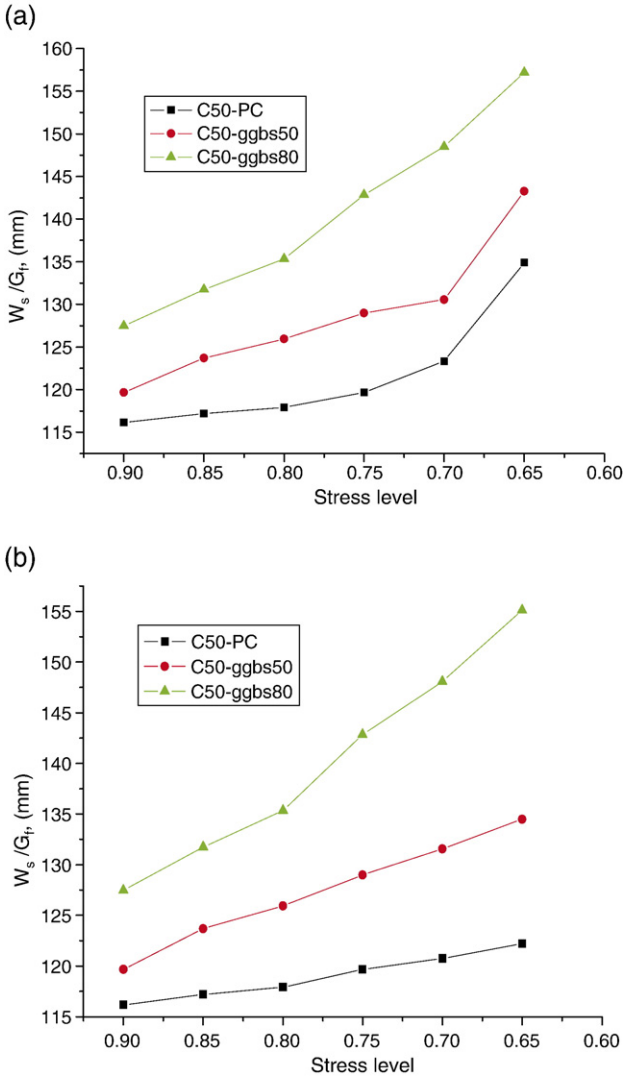

Fig. 7. W_s/G_f and stress level relations for three concrete series. (a) Experimental results; (b) GM (1, 1) forecast results.

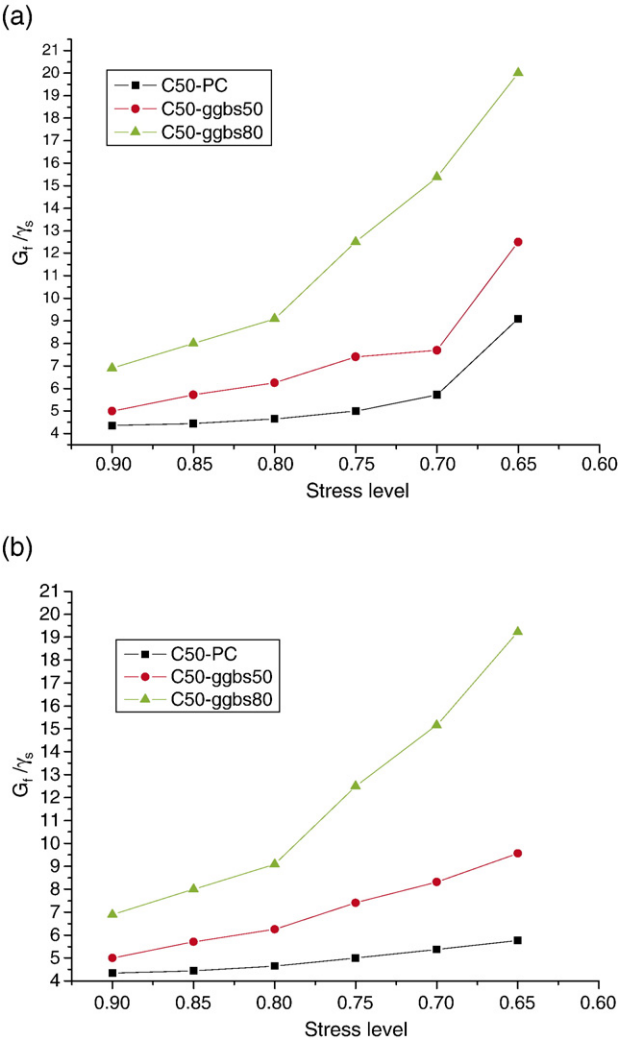

Fig. 8. G_f/γ_s and stress level relations of three concrete series. (a) Experimental results; (b) GM (1, 1) forecast results.

4.6. Two forms of fracture energy

4.6.1. Fracture energy based on surface macro-crack

The majority of fracture energy was dissipated by the propagation of surface macro-cracks [1,15,16]. The sources of fracture energy are different as varying the stress levels. With the results of fractal dimensions of surface cracks, the fracture energy equation was established based on surface macro-crack.

According to [1], at the nth scale of the fractal crack, the total energy W_s dissipated at the surface of the crack in a plate of unit thickness is given by

$$W_s = G_f a \tag{22}$$

Where G_f is the fracture energy of concrete at the scale of observation δ. a is the *Euclidean* length which should be

modified by fractal theory. By substituting $a^* = a\left(\frac{\delta}{a}\right)^{1-D_{1-d}}$ for a, the above equation is then

$$W_s = G_f a^* = G_f a\left(\frac{\delta}{a}\right)^{1-D_{1-d}} \tag{23}$$

$$\frac{W_s}{G_f} = a\left(\frac{\delta}{a}\right)^{1-D_{1-d}} \tag{24}$$

In this paper, when a is equal to height of cross-section and δ is equal to 5 mm, the fracture energies based on surface macro-cracks were come out and presented in Fig. 7.

4.6.2. Fracture energy based on fractured profile

The classical equation to calculate G_f is established by the committee of FILEMTC50-FMC [17,18].

$$A = B \cdot H \tag{25}$$

$$G_f = W/A \tag{26}$$

Wherein, B is the height, H is the width, W is the total dissipated power in process of fatigue fracture. A in above equation is a *Euclidean* area, which is not accurate to descript the coarse content of ruptured surface.

The total power dissipated by rupture surface during the flexure fatigue process is defined as

$$W = 2\gamma_s \cdot A_s = 2\gamma_s \cdot HB\left(\frac{\delta^2}{HB}\right)^{2-(D_H+D_B)} \tag{27}$$

Wherein, γ_s is the surface energy density of concrete. Therefore, the fracture energy of fractured profile is

$$G_f = \frac{W}{BH} = 2\gamma_s\left(\frac{\delta^2}{HB}\right)^{2-(D_H+D_B)} \tag{28}$$

or

$$\frac{G_f}{\gamma_s} = 2\left(\frac{\delta^2}{HB}\right)^{2-(D_H+D_B)} \tag{29}$$

where 100 mm is chosen as the value of H and B. δ is 5 mm. The experimental results and GM (1, 1) forecast results are plotted in Fig. 8.

It is obvious that the high proportions of ggbs are a benefit for concrete to improve the flexural fatigue performance. For each series of concrete, the fracture energy increases as the stress level decreasing. And at the same stress level, the experimental results of concrete with high proportions of ggbs are greater than those of C50-PC. It is proved that greater fractal energies of concretes with ggbs are dissipated in fractured profile during the flexural fatigue process because of more zigzag surface macro-cracks and more complicated fractured profiles. They are consistent with all of experimental results in above sections.

5. Conclusion

- The fatigue life of C50-ggbs50 and C50-ggbs80 is longer than those of C50-PC. As the stress level is equal to or higher than 0.80, C50-ggbs50 has the longest fatigue life in three series. Nevertheless, the fatigue life of C50-ggbs80 is the longest as the stress levels lower than 0.80.
- In order to investigate the flexural fatigue mechanism of three series of concretes, five fractal parameters (i.e. D_{1-d}, A_s, R_B, P_{DA} and G_f) were established to describe the positive effect of ggbs in concrete matrix. It is obvious that ggbs incorporated in matrix can impair the brittleness, increase the fracture energy and prolong the fatigue life of concrete. Specially, the effect of ggbs on concrete is more obvious at the lower stress levels.
- The GM (1, 1) is an effective tool to inspect effectively the experimental results on-line. It will reduce testing time greatly.
- The flexural fatigue experiment results show that the concretes with high mass fractions of ggbs in matrix are adapt to be utilized as protection layer of reinforcements in concrete structures exposed to cyclic stress, e.g. highway slabs, bridges, railway sleepers and airfield pavements.

Acknowledgments

The research was supported by the National Natural Science Foundation of China (Grant No. 59938170), the foundation for Excellent Doctoral Dissertation of Southeast University of China, and the fund from China Scholarship Council. The authors gratefully acknowledge Jiangsu Bote New Materials Co., Ltd. of China providing hydraulic fatigue machine.

References

[1] Andrea Carpinteri, Andrea Spagnoli, A fractal analysis of size effect on fatigue crack growth [J], International Journal of Fatigue 26 (2004) 125–133.
[2] L.T. Dougan, P.S. Addison, W.M.C. McKenzie, Fractal analysis of fracture: a comparison of dimension estimates [J], Mechanics Research Communications 27 (4) (2000) 383–392.
[3] Xiaoyan Liu, et al., Application to fractal theory in study on the fracture surfaces of concrete [J], Journal of China Three Gorges University (Natural Sciences) 25 (6) (2003) 495–499 (in Chinese).
[4] K. Ganesh Babu, V. Stree Rama Kumar, Efficiency of GGBS in concrete [J], Cement and Concrete Research 30 (2000) 1031–1036.
[5] J.C. Maso, Interface transition zone in concrete [M], RILEM Report, vol. 11, St Edmundsbury Press, Great Britain, 1996, pp. 103–115.
[6] J.L. Deng, Introduction to grey system theory [J], Journal of Grey System 1 (1) (1989) 1–24.
[7] J.L. Deng, Properties of multivariable grey model GM (1 N) [J], Journal of Grey System 1 (1) (1989) 125–141.
[8] J.L. Deng, Control problems of grey systems [J], System Control Letters 1 (1) (1989) 288–294.
[9] M.Z. Mao, E.C. Chirwa, Application of grey model GM (1, 1) to vehicle fatality risk estimation [J], Technological Forecasting & Social Change 73 (2006) 588–605.
[10] Heping Xie, et al., Fractal Geometry—Mathematic Foundation and Application [M], Chongqing University Press, Chongqing, 1991, pp. 189–196, in Chinese.
[11] Yu Chen, et al., Application of fractal theory in concrete destructive surfaces and discussion of fractal dimension calculating methods [J], Concrete 10 (2004) 18–21 (in Chinese).

[12] Mohsen A. Issa, Mahmoud A. Issa, et al., Fractal dimension a measure of fracture roughness and toughness of concrete [J], Engineering Fracture Mechanics 70 (2003) 125–137.
[13] An Yan, et al., Relationship between brittleness and characterization of fracture surface for high strength concrete [J], Journal of Tongji University 30 (1) (2002) 66–70 (in Chinese).
[14] Jun Zhang, et al., Conditions promoting crack growth in concrete along the aggregate/matrix interface or into the aggregate [J], Journal of Tsinghua University (Science and Technology) 44 (3) (2004) 387–390 (in Chinese).
[15] Z.P. Bazant, et al., Fracture and Size Effect in Concrete and other Quasibrittle Materials [M], CRC Press LLC, 1998.
[16] Wei-Tao Li, et al., Theory of fractal applied to concrete study [J], Journal of Hebei University of Technology 32 (6) (2003) 13–16 (in Chinese).
[17] G.I. Barenblatt, et al., Incomplete self-similarity of fatigue in the linear range of crack growth [J], Fatigue Fracture Engineering Material Structure 3 (1980) 193–202.
[18] A.I. Carpinteri, Scaling laws and renormalization groups for strength and toughness of disordered materials [J], International Journal of Solids Structure 31 (1994) 291–302.